Article:

Agbotui, PY, West, LJ orcid.org/0000-0002-3441-0433 and Bottrell, SH (2020) Characterisation of fractured carbonate aquifers using ambient borehole dilution tests. Journal of Hydrology, 589. 125191. ISSN 0022-1694

https://doi.org/10.1016/j.jhydrol.2020.125191

TITLE: **Characterisation of fractured carbonate aquifers using ambient borehole dilution tests**

Prodeo Yao Agbotui[1,2], Landis Jared West[1], Simon Henry Bottrell[1]

[1] School of Earth and Environment, University of Leeds, Woodhouse Lane, Leeds, West Yorkshire, LS2 9JT, United Kingdom. Author email addresses: ee08pya@leeds.ac.uk; l.j.west@leeds.ac.uk; s.bottrell@leeds.ac.uk

Corresponding author: Landis Jared West, email address l.j.west@leeds.ac.uk, correspondence address: School of Earth and Environment, University of Leeds, Woodhouse Lane, Leeds, West Yorkshire, LS2 9JT, United Kingdom

[2] Permanent Address: Department of Civil Engineering, Accra Technical University, Accra Central, Ghana, West Africa

Abstract

Fractured carbonate aquifers derive their transmissivity essentially from a well-developed network of solutionally-enhanced fractures and conduits that can lead to high groundwater velocities and high vulnerability to contamination of water quality. Characterisation of the variation of hydraulic properties with depth is important for delineating source protection areas, characterising contaminant fate and transport, determination of the effectiveness of aquifer remediation, and parameter estimation for models. In this work, ambient open borehole uniform and point injection dilution tests were conducted on observation boreholes in the unconfined Cretaceous Chalk aquifer of East Yorkshire, UK, and interpreted in conjunction with other data via the implementation of a new work flow. This resulted in the characterisation of flow in these boreholes and the inference of properties such as groundwater flow patterns and velocities in the surrounding aquifer formation. Our workflow allowed sections of open boreholes showing horizontal versus vertical flow to be distinguished, and the magnitude of such flows and exchanges with the aquifer to be determined. Flow within boreholes were then used to characterise: i) presence and direction of vertical hydraulic gradients; ii) nature and depth distribution of flowing features; iii) depth interval porosity and permeability estimation of the flowing features from overall borehole transmissivity and geophysical image or caliper logs; iv) groundwater velocity estimation in the surrounding aquifer. Discrete flowing features were distributed across the range of depths sampled by the observation boreholes (typically up to 45 to 60 mbgl), but the majority were located in the zone of water table fluctuation marked by solutionally enlarged flow features. Quantitative interpretation of both uniform injection (tracer distributed throughout the open borehole section) and point injection (slug of tracer introduced at targeted depth) yielded vertical velocities within the borehole water column in broad agreement with those measured by flow logging. Depth specific fracture kinematic porosities inferred from the ambient dilution data combined with long-interval pump test and geophysical log data ranged between $3.7 \times 10^{-4} – 4.1 \times 10^{-3}$ with an average of 2.1×10^{-3}; these values were in excellent agreement with those from other methods applied to the same aquifer such as larger scale pumping tests. A new

approach to estimation of groundwater velocities from the dilution test data using externally measured hydraulic gradients gave inferred horizontal groundwater velocities ranging between 60 – 850 m/day, in full agreement with those from previously conducted borehole-to-borehole tracer tests. These results confirm that the studied aquifer is karstic, with rapid preferential pathways which have implication for flow and transport modelling, and pollution vulnerability. Our study results indicate that ambient single-borehole dilution approaches can provide an inexpensive and reliable approach for the characterisation of fractured and karstic aquifers.

Keywords: Fractured aquifer, borehole dilution, tracer tests, wellhead protection, carbonate, aquifer vulnerability.

1. Introduction

Preferential flowpaths and vertical head gradients are pervasive in fractured rock aquifers (Singhal and Gupta, 1999; Cook, 2003). Knowledge of fracture and conduit connectivity and vertical hydraulic gradients are important for aquifer characterisation and developments such as: the design and development of abstraction boreholes, targeted horizon sampling for chemical characterisation (Moir et al., 2014; McMillan et al., 2014), groundwater flow interpretation and modelling (Saines, 1981; Brassington, 1992; Dalton et al., 2006; Weight, 2008) and effective design of remediation schemes. Methods for characterising preferential flowpaths in fractured aquifers can be classified as catchment scale and single borehole methods (Singhal and Gupta, 1999; Cook, 2003). Catchment scale tests include stream sink point-to-spring and ambient borehole-to-borehole tracer tests (Cook, 2003; Bottrell et al., 2010). These give direct measurement of groundwater velocity and fracture connectivity. However, catchment scale tracer tests are expensive and difficult to set up. Cheaper single-borehole characterisation approaches include core sampling (Shuter and Teasdale, 1989), conventional geophysical logging (Keys, 1990), caliper logging (Paillet and Pedler, 1996), borehole CCTV (Zemanek et al., 1970; Paillet, 1991), packer testing (Quinn et al., 2011), flow logging (Molz et al., 1989; Parker et al., 2010), and single borehole dilution testing (Tsang et al., 1990; Tsang and

Doughty, 2003; West and Odling, 2007; Maurice et al., 2010; Parker et al., 2010), amongst others. Core logging and sampling can be problematic for carbonate aquifers where flow is dominantly in fractures and conduits, due to inability to preserve fracture properties in the recovered core. Conventional borehole geophysical techniques use the borehole wall or fluid properties such as neutron, gamma and resistivity logging, and caliper logs to measure borehole wall enlargements which often coincide with fractures (which may or may not be flowing features). Borehole CCTV and image logs provide a view of borehole wall properties by showing fractures, but not all fractures detected are flowing features. Borehole fluid flow logging under pumped and or ambient conditions and/or packer tests are typically used to evaluate hydraulic conductivity and flow variation with depth (Day-Lewis et al., 2011; Parker et al., 2010; Medici et al., 2018; Quinn et al., 2011). In impeller flow logging, increase or decrease in borehole vertical flows within a logged interval is used to infer inflow or outflow to the aquifer respectively. However, impeller flow logging is expensive, and is insensitive to small ambient flows (Pitrak et al., 2007). Impeller flow logging is also not able to detect horizontal crossflows in boreholes (Paillet and Pedler, 1996; Maurice et al., 2010). In packer testing, sealing in open boreholes in fractured formations often presents difficulties because of wall irregularities, and skin effects may cause errors in hydraulic conductivity estimation. Also, hydraulic conductivity estimation requires assumptions about the shape of the flow field which are based on granular aquifers and nearly always wrong in fracture flow systems (Boulding, 1993; Singhal and Gupta, 1999). Furthermore, packer tests sample only a small volume of the aquifer near the borehole wall except where they are conducted on intervals with highly transmissive fractures (Paillet et al., 2012). In contrast, single borehole dilution testing characterises hydraulic properties by interpreting the tracer concentration profile development resulting from inflowing formation water. Compared to other borehole characterisation techniques, single borehole dilution is not only relatively easier to set up, but is also highly sensitive to low ambient flows in boreholes. It can also detect crossflows. Improved interpretation is possible when combined with data from image and caliper logs (Kobr, 2003; Maurice et al., 2010). Tsang et al. (1990), Kobr (2003), Doughty et al. (2005), Doughty et al. (2008), Datel et al. (2009) and Maldaner et al. (2018) found good agreement between single borehole dilution interpretations and those from other single borehole characterisation methods like core logging, packer and slug testing, flow logging and conventional geophysical logging.

Extending single borehole dilution test interpretation to the catchment scale would reduce investigation cost, and remove the difficulty and uncertainty associated with the performance of borehole-to-borehole tracer tests. However, there are few published examples where ambient single borehole tests are validated by catchment scale measurements. Novakowski et al. (2006) for instance used ambient borehole-to-borehole tracer tests to validate single borehole dilution tests in limestone and dolostone aquifers in Ontario, Canada. In that work the single-borehole method used was more expensive than that used in our study described in this paper, in that packers and standpipes were installed in the boreholes. However, their study successfully showed that single borehole dilution tested fractures that were conductive at the catchment scale had comparable fracture hydraulic gradients to the regional hydraulic gradient and also had same order of magnitude fracture velocities to groundwater velocities from natural borehole-to-borehole tracer tests. In contrast, hydraulic gradients and fracture velocities of local fractures were dissimilar to that from borehole-to-borehole tracer tests.

In this work we develop the ambient single borehole dilution tests approach and validate the results against other methods (single borehole optical, caliper logging and borehole flow logging and borehole-to-borehole tracer testing). We present a new workflow which involves determination of flowing horizons and dominant flow mechanisms from single-borehole dilution data, followed by application of quantitative analysis to both uniform injection and point injection test results. The new workflow is applied to a series of ambient single borehole dilution tests performed in four boreholes in the Kilham Catchment of the East Yorkshire Chalk Aquifer, United Kingdom: a fractured carbonate aquifer. Via the implementation of a new methodology and decision process, boreholes dominated by either horizontal or vertical flows were identified. In cases where vertical flow in the borehole water column dominated, vertical borehole fluid velocities and tracer mass losses were quantified. In cases where horizontal flows dominated, groundwater velocities in the surrounding aquifer were found combined with the regional hydraulic gradient. In each case, the single-borehole test data was used to inform a conceptual model of flow in the aquifer at the borehole-test scale. Borehole-test scale groundwater velocities were then validated against those inferred from borehole-to-borehole tracer tests.

2. Theoretical development and analytical concepts

2.1 Single borehole dilution tests and analytical methods

Single borehole dilution testing is a technique used to characterise borehole hydraulic properties and flow variation with depth in open boreholes in aquifer formations (i.e. $K > 10^{-6}$ m/s, Pitrak et al., 2007) often via monitoring specific electrical conductance (SEC) contrasts between aquifer formation fluid and borehole fluid column following the introduction of a tracer in the borehole (Tsang et al., 1990; Pedler et al., 1990; Pedler et al., 1992; Kobr, 2003; West and Odling, 2007; Maurice et al., 2010; Paillet et al., 2012). Single borehole dilution testing can be undertaken under pumped (eg. Brainerd and Robbins, 2004; Pedler et al., 1992; Tsang et al., 1990; West and Odling, 2007) or ambient (eg. Drost et al., 1968; Lewis et al., 1966; Maurice et al., 2010) conditions, using either uniform and point injection approaches. In uniform injection, the entire section of the borehole that is open to the aquifer is injected with a tracer. Horizontal flow across the borehole is indicated by proportional tracer dilution with time, whereas vertical flow in the borehole is depicted by movement of the boundary of the tracer and inflowing formation water along the vertical axis of the borehole. In point injection, a tracer slug is injected at a targeted depth, and the tracer slug is monitored for vertical movement and mass loss along the axis of the borehole.

The single borehole dilution method has advantages as compared to other borehole investigation techniques. The method is sensitive to very low ambient flows that cannot be resolved by impeller flowmeters (Tsang et al.,1990;West and Odling, 2007) and can also detect crossflows under both ambient and pumped conditions (Doughty and Tsang, 2005; West and Odling, 2007; Maurice et al., 2010). It is also less expensive in relation to packer tests (Tsang et al., 1990; Tsang and Doughty, 2003; West and Odling, 2007) and flowmeter logging (Tsang et al., 1990; Pedler et al., 1990). However, correct interpretation of single–borehole test data requires that tracer dispersion within the borehole water column is distinguished from the effects of tracer dilution by inflows from flowing features and mass loss through outflows (Brainerd and Robbins, 2004; West and Odling, 2007). Secondly, borehole dilution tests are not suitable for characterising non-aquifers because processes like diffusion, density driven flows and probe signal artefacts can dominate over those modelled by tracer dilution (Ward et al., 1998).

Common tracers used for the single borehole dilution testing include NaCl (West and Odling, 2007; Maurice et al., 2010; Moir et al., 2014), deionised water (Pedler et al., 1990; Tsang et al., 1990), fluorescein (Lewis et al., 1966) and food dyes (Pitrak et al., 2007). NaCl was chosen as a tracer for this work because it is inexpensive, readily available, easy and safe to handle and non-toxic to humans and the environment and can be monitored via SEC signature (Ward et al., 1998). Note that in very rapid flow conditions, EC measurements may become inaccurate and other tracers such as fluorescein or food dyes may be preferable (Pitrak et al., 2007). Also NaCl concentration > 120 g/L can cause density driven flows (Ward et al., 1998).

Generally, the single borehole dilution test is analysed and interpreted from the tracer concentration difference between initial injection time and subsequent times as a result of influx and mixing with fresh formation water diluting the tracer. The analytical techniques for analysing single borehole dilution tests are based on mass conservation theories and the solution to solute transport models such as the 1-dimensional advection dispersion equation (ADE). The ADE models the rate of change of tracer concentration in the borehole water column with respect to time (West and Odling, 2007):

$$\frac{\partial \mathrm{C}(\mathrm{z},\mathrm{t})}{\partial \mathrm{t}} = -\frac{\partial\big(\mathrm{Cu}(\mathrm{z},\mathrm{t})\big)}{\partial \mathrm{z}} + \frac{\partial}{\partial \mathrm{z}}\left[\alpha_{\mathrm{B}}\mathrm{u}(\mathrm{z},\mathrm{t})\frac{\partial \mathrm{C}}{\partial \mathrm{z}}\right] - \frac{\mathrm{CQ_o}(\mathrm{z},\mathrm{t})}{\pi r_w{}^2} \qquad (1)$$

where C(z,t) is the concentration at time t after tracer injection at elevation z, u(z,t) is vertical fluid velocity in the borehole, $Q_o(z,t)$ is the volumetric inflow rate of formation water of zero tracer concentration per unit depth of borehole per unit time, r_w is the borehole radius, and α_B is the coefficient of dispersivity in the flow direction (i.e. vertical). The first term on the right of Equation (1) represents vertical advective effect of the flow in the borehole. The second term describes vertical 'Fickian' dispersion of tracer. The last term represents dilution effect of inflowing formation water and loss of tracer from outflow. The assumptions are thus that dispersion within the borehole water column is Fickian, i.e. the solute distribution is Gaussian; borehole diameter is small compared to the length which allows full mixing between the inflowing and the borehole water at each depth interval; and density-driven effects are negligible in the borehole. Mass conservation implies that both water discharge and solute mass entering a fracture or set of fractures is equal to the difference in vertical flow and mass flux in the borehole above and below these fractures (Tsang et al., 1990; Brainerd and Robbins, 2004; Doughty and Tsang, 2005).

Methods for analysing single borehole dilution test data include: the 'signature' method, analytical, modelling/curve fitting and combined techniques. The signature approaches give a qualitative interpretation and understanding of flow processes in boreholes from the analyses of various features created by inflow, outflow, crossflow and vertical flow on temporal tracer profiles (Doughty and Tsang, 2005; Maurice et al.,2010). Signature approaches are simple to use but are subjective and sometimes produce non-unique interpretation (Doughty and Tsang, 2005; Maurice et al.,2010). Quantitative analytical methods use the mass balance of solute to infer flow properties for pumped-borehole dilution tests (Tsang et al., 1990), and for the specific case of horizontal crossflow in ambient conditions (Drost et al., 1968; Lewis et al., 1966; Ward et al., 1998; Pitrak et al., 2007). The analytical techniques provide useful information when used in conjunction with other types of complementary analyses, but on their own are overly simplistic for real world problems (Doughty and Tsang, 2005;

Ward et al., 1998). These modelling approaches fit the field SEC profile to, for example, the 1-D ADE model (Doughty and Tsang, 2005; West and Odling, 2007) by specifying flowing feature elevations and varying the discharge and solute concentration at the fracture (BORE codes, I & II in Tsang et al., 1990), or varying flow velocity and vertical dispersivity in the borehole until there is a good fit between the field data and the ADE (West and Odling, 2007). Combined approaches model the tracer profile development using both the signature and analytical techniques to constrain flow characteristics in the borehole (Doughty and Tsang, 2005; Maurice et al.,2010). They are simple to use, more efficient and require less time and effort, and provide a better constraint on flow in boreholes (Doughty and Tsang, 2005; Moir et al., 2014). In this work, we focus on the combined approach for analysing single borehole dilution tests in ambient flow conditions.

Analysis approaches for ambient-flow open borehole dilution tests in a fractured aquifer like the Chalk assume that flow occurs via discrete horizons (Singhal and Gupta, 1999; Cook, 2003). Due to hydraulic head differences between the layers, recharge and discharge areas of the aquifer are often dominated by vertical flows. In transition zones between recharge and discharge areas, where head gradients between flowing features are small, horizontal crossflows often dominate. In some areas, a combination of vertical and horizontal flows can be present within a single borehole water column (Toth, 1962; Freeze and Witherspoon, 1968; Brassington, 1992; Toth, 2009; Liang et al., 2010). Single borehole tracer signatures produced from horizontal crossflow versus vertical flows are presented in detail in Doughty and Tsang (2005) and Maurice et al. (2010).

For the case of borehole sections dominated by horizontal crossflow, the horizontal specific discharge can be found assuming that: the concentration across the borehole water column is uniform (ie well mixed), there are no vertical flows and that flow is steady-state; then the first and second terms of equation (1) are negligible. Integrating (1) and using the boundary conditions of C from C_o to C_t, and time from 0 to time, t and re-arranging yields:

$$InC_t = -\left(\frac{2q_w}{\pi r_w}\right)t + InC_0 \qquad (2)$$

where $q_w = \alpha q_f \qquad (3),$

where q_w is the horizontal specific discharge or Darcian flux through the borehole interval, q_f is the formation specific discharge, α is the dimensionless flow constriction factor that accounts for flow convergence and distortion from the formation into the open section of the borehole (Drost et al., 1968; Gustafsson and Anderson, 1991), defined by the ratio of the aquifer width contributing to flow to the borehole to the borehole diameter, and C_t is concentration at any time t after injection of tracer.

Plotting the natural logarithm of concentration versus time at depth of interest produces a linear response (hereon referred to as the Pitrak et al. (2007) method), with the slope, m of the tracer decay line proportional to q_w i.e.:

$$q_w = \frac{m\pi r_w}{2} \qquad (4).$$

Finding q_f using eqn (2) and dividing by ϕ_e, the fracture kinematic porosity, yields the average linear velocity of groundwater in the formation v_{fh}:

$$v_{fh} = \frac{q_f}{\phi_e} = \frac{q_w}{\alpha\phi_e} = \frac{m\pi r_w}{2\phi_e\alpha} \qquad (5).$$

Constraining the values of α and ϕ_e are the main difficulty in using equation (5). The flowing fracture porosity ϕ_e can be estimated from hydraulic tests, and the number of flowing fractures intersecting the borehole interval from geophysical logging, by assuming the cubic law for parallel fractures, see section 2.2 below (Novakowski et al., 2006; Quinn et al., 2011; Maldaner et al., 2018; Medici et al., 2019).

For the case of borehole sections with dominant ambient vertical flows, equation (2) is not applicable because of vertical flow effects (Drost et al., 1968; Ward et al., 1998; Pitrak et al., 2007; Piccinini et al., 2016). In that case, tracer will travel vertically along the borehole with dilution and/or mass loss from inflow and outflow/crossflow features respectively (Maurice et al., 2010). The mass of solute under any concentration profile is given (Doughty and Tsang, 2005) as:

$$M = \int [C(z) - C_0]\pi {r_{wa}}^2 dz \qquad (6)$$

In equation (6), r_{wa} is the average borehole radius from caliper log. Applying equation (6) to ambient flow uniform injection test data is difficult due to possible dispersion and interference of flowing feature signatures. However, for the case of point injection of a tracer slug at a discrete depth, comparison of sequential profile M values indicates where mass is conserved (no outflow) versus lost (outflow), and comparison of masses above and below flowing features indicates the extent of tracer mass lost. Furthermore, sequential profile centroid positions can be used to estimate velocity of vertical flow, u. Using the profile velocities and borehole radius from caliper logs where available, vertical discharge Q_v is computed (Kobr, 2003) as:

$$Q_v = \pi {r_{wa}}^2 u \qquad (7)$$

Using the mass integrals under the profiles and the differences between Q_v for adjacent borehole sections, the magnitude of borehole inflows and outflows associated with specific flowing features or intervals are constrained. This approach informs the development of conceptual models of flow for each tested borehole.

2.2 The parallel plate model (cubic law)

In a borehole intersected by fractures, flowing fracture aperture, a_f can be found from the fracture transmissivity T_f using the parallel plate model, also called the cubic law (Snow, 1969; Witherspoon et al., 1980; Qian et al., 2011):

$$a_f = \sqrt[3]{\frac{12\nu T_f}{g}} \qquad (8)$$

where ν and g are the kinematic viscosity of water (1.307 x 10^{-6} m^2s^{-1}) and acceleration due to gravity, (9.81 ms^{-2}) respectively. T_f is the single aperture transmissivity, and is defined as:

$$T_f = \frac{T_i}{N_i} \qquad (9)$$

where T_i is the transmissivity of the borehole interval (i.e. vertical section of borehole) and N_i is the number of flowing features intersecting that interval e.g. identified from geophysical and core logging.

The effective fracture porosity ϕ_e for the formation intersected by the interval with length L can thus be determined as:

$$\phi_e = \frac{N_i \, a_f}{L} \qquad (10)$$

As an alternative to equation (5), the average horizontal velocity of groundwater in the formation intersected by the borehole interval can also be found using the regional hydraulic gradient i_f together with the fracture aperture a_f

$$v_{fh} = k_f . i_f = \frac{(a_f)^2 g}{12\nu} i_f \qquad (11)$$

where k_f and i_f are the fracture hydraulic conductivity and hydraulic gradient in the formation surrounding the borehole respectively. The assumptions for using equations (8) to (11) to find the average horizontal groundwater velocity in the formation are that the flowing features intersecting the interval are horizontal or shallowly dipping fractures with equal transmissivity and hence hydraulic aperture implying that:

$$k_f = \frac{T_f}{a_f} \qquad (12)$$

Groundwater velocities have been derived from single borehole tests undertaken by previous workers who either used straddle packers (Novakowski et al., 1995; Xu et al., 1997; van Tonder et al., 2002; Novakowski et al., 2006; Akoachere and Van Tonder, 2009; Maldaner et al., 2018) or depth specific piezometers (Piccinini et al., 2016; Medici et al., 2019) to isolate borehole sections. In this paper, we combine this approach with borehole dilution tests to determine the variation in effective fracture porosity with depth for long open borehole sections. We compare groundwater velocities derived from single borehole tests with those from borehole-to-borehole tracer tests in order to validate the method.

3. Study area

The aquifer on which the study area is located is the unconfined area of the Cretaceous Chalk aquifer in East Yorkshire, NE England, UK (Figure 1). In the United Kingdom (UK), the Chalk is the most important aquifer, providing about 60% of public water supply contributed by groundwater (Allen et al., 1997; Downing, 1998; Knapp, 2005). In East Yorkshire, the Chalk is the main source of potable water supply for domestic and industrial supplies (Edmunds et al., 2001; Smedley et al., 2004; Gale and Rutter, 2006). The Chalk also supports the ecology and the conservation Sites of Special Scientific Importance (SSSI) of the River Hull, the headwaters of which are groundwater fed (Gale and Rutter, 2006). The Chalk aquifer lies uncomfortably over Jurassic Formations with the main aquifer units being the Flamborough, Burnham and Welton Formations. The bedding dips at 2° to the south-east. The Chalk aquifer derives its high transmissivity from a well-developed network of solutionally-enhanced joints, faults, bedding plane features and karst conduits or channels (Allen et al., 1997; Bloomfield, 1996). The joints are steeply dipping, the majority of which are stratabound, with joint spacing ranging between 0.3 – 0.5 m. Joint trace lengths range between 0.65 – 2.5 m. Bedding plane fractures are persistent laterally, making bedding plane fractures the main flowpaths for groundwater flow and contaminant transport (Bloomfield, 1996; Waters and Banks, 1997). Thin marl layers act as barriers to vertical flow, thereby concentrating flows along bedding fractures (Gale and Rutter, 2006), causing solutionally enhanced bedding-parallel flow features (widened fractures and small conduits). Although the Chalk is a dual porosity aquifer, effective storage for the aquifer is from the fracture network as the narrow pore throats (0.1 to 1.0 µm) within the Chalk matrix prevent drainage from the matrix (Price, 1987; Price et al., 2000).

Despite the importance of the Chalk as an aquifer, since the 1970s it has been plagued by contamination from nitrate and other agrochemicals resulting in several studies to characterise: resource assessment (Foster and Milton, 1974; Foster and Milton, 1976; Jones et al., 1993), hydraulic conductivity variation with depth (Buckley and Talbot, 1994; Bloomfield, 1996; West and Odling, 2007; Parker et al., 2010; Parker et al., 2019), borehole-to-borehole tracer tests for the delineation of the source protection zone (SPZ) areas for boreholes and springs (Ward and Williams, 1995; Ward et al., 2000). The four boreholes tested here using ambient single borehole dilution tests are Field House Farm, Kilham (FHK), Little Kilham Farm (LKF), Tancred Pit (TP) and Weaverthorpe (WTP), see Figure 1. In all the boreholes, the upper parts of the boreholes are cased, with open sections below. Table 1 shows the borehole details and their injection parameters. Note that the connectivity and horizontal groundwater velocities between boreholes, Henpit Hole (HPT 1 & 2) and Middledale borehole (MD) & LKF borehole were previously established using borehole-to-borehole tracer tests (see Figure 1)

Table 1

Borehole details and injection parameters of single borehole dilution tests in this study

Borehole name	UK national grid reference	Ground elevation (m AoD)	Borehole top diameter (mm)	Borehole depth (m)	Depth of open section tested (m)	Type of single borehole dilution test conducted		Mass of salt injected in tests (g)	
						Uniform	Point	Uniform	Point
Field House Kilham (FHK)	TA 071 672	68.66	208	67	24	Yes	No	450	N/A
Little Kilham Farm (LKF)	TA 046 649	39.96	202	50	32	Yes	Yes	900	75
Tancred Pit (TP)	TA 069 660	36.40	220	50	37	Yes	Yes	2500	75
Weaverthorpe (WTP)	SE 981 702	71.00	152	46	19	Yes	Yes	650	75

4. Methods

4.1 Single-borehole dilution tests set up

Both uniform injection (Ward et al.,1998; Pitrak et al., 2007; Maurice et al., 2010) and point emplacement (Tate et al., 1970; Kobr, 2003; Maurice et al., 2010) ambient flow single-borehole dilution tests were undertaken (Figure 2 and Table 1). Groundwater levels at the time of each test are marked on the respective figures; these were essentially similar between the different types of test. The borehole was first logged for background specific electrical conductivity (SEC) with a Solinst TLC dipper at specific depth intervals. For the uniform injection tests (Figure 2.a), NaCl solution was injected uniformly into the boreholes by filling a 25 mm diameter weighted hose ({NaCl} ≤ 120 gL^{-1} in hose) inserted into the borehole. The hose pipe was slowly pulled out of the borehole to produce initial uniform tracer concentration via mixing with the borehole water. Then sequential logs of SEC ($\mu S/cm$) with depth were measured and converted to sodium chloride concentrations {NaCl} (g/L) using a calibration equation (signal SEC = 1714.5 {NaCl} + 464, R^2=0.99) derived from dissolving known masses of NaCl in Chalk water and measuring the resulting SEC signal. The work flow in Figure 3 was implemented to characterise the borehole as horizontal or vertical flow dominated and for targeting depths for point injection tests. For point injection tests (Figure 2.b), target injection depths were injected with 0.5L of 150 gL^{-1} NaCl solution (i.e. 75g of NaCl) from a 1.2 m long x 70 mm diameter point injection barrel. The barrel was then dropped to the target depth and released by operating a connected Rothenberger Test pump at the ground surface. Sequential SEC measurements were made to monitor vertical migration and attenuation of the resulting sodium chloride slug within the borehole.

4.2 Single-borehole dilution test work flow and interpretation process

Figure 3 shows the workflow and decision tree for the interpretation of single-borehole dilution tests. Following signature / qualitative analyses of uniform injection tests, the method of Pitrak et al. (2007) (refer to section 2.1) was applied to the uniform injection test data to verify whether or not flow at each monitored depth interval was dominated by vertical or horizontal flow. For boreholes dominated by lateral horizontal flows, the analysis yields horizontal specific discharge versus depth. For such cases (“Yes” decision route in Figure 3), specific discharge data were combined with geophysical log and hydraulic test transmissivities and external hydraulic gradients by implementing equations 8-11 (parallel plate model) to produce fracture effective porosity and horizontal fracture flow velocities versus depth. For vertical flow dominated boreholes (“No” decision route in Figure 3), point injection tests at targeted depths were analysed via plotting centroid velocity, tracer mass loss) and vertical flow rate differencing at sequential sections of the borehole. Where possible methodologies described in Doughty and Tsang (2003), Kobr (2003) and Maurice et al. (2010) were applied to find inflow and outflow fluxes into discrete fractures/intervals from the observed changes in vertical borehole flows.

5. Results and interpretation

5.1 Results

5.1.1 Uniform injection tests

The results of uniform injection tests are shown in Figure 4. FHK borehole diameter (Figure 4.a(i)) is regular with two minor enlargements between depths 50 - 55 mbgl. The initial tracer concentration (Figure 4 a(ii)) ranged between 0.85 – 0.99 gL^{-1}, with a freshwater front slowly progressing downwards from the water table reaching >60 mbgl by 2178 minutes.

The WTP borehole (Figure 4.b (i)) borehole optical image log shows horizontal and sub-horizontal feature traces distributed at different depths, coinciding with borehole enlargement on the caliper log (Figure 4.b (ii)). The borehole diameter is irregular ranging in diameter from 100 and 155 mm, with the diameter enlargements occurring between depths 25 and 37 mbgl. The WTP uniform injection test (Figure 4.b (iii)) show an initial salt concentration of 2.75 gL^{-1} (preserved only near the borehole bottom and near the water table), with very large distinctive concentration falls (kink points) at 33.5 and 40 mbgl persisting through the test. A freshwater front drives tracer up the borehole from the kink point at 40 mbgl, with the tracer peak moving progressively upwards to the kink point at 33.5 mbgl. Above 33.5 mbgl tracer dilution is more uniform but less rapid; dilution is relatively slow below the kink point at 40 mbgl, with little dilution below 42 mbgl.

The TP borehole diameter (Figure 4.c(i)) is highly irregular, ranging between 200 and 480 mm, with diameter enlargement occurring between depths 14.5 and 29 mbgl. The uniform injection (Figure 4.c(ii)) test shows a rapid dilution of tracer, suggesting upward moving freshwater front from the borehole bottom exiting near the base of the casing at 13 mbgl, reaching 22 mbgl within 20 mins (first profile; all subsequent profiles show background concentration).

The LKF borehole diameter (Figure 4.d (i)) is irregular, ranging from 225 – 460 mm with the majority of the largest diameters occurring between depths 15m and 26 mbgl. LKF uniform injection data (Figure 4.d (ii)) show a fairly uniform initial concentration (~1.4 gL^{-1}) was achieved below 27 mbgl, but by the time of the first profile (5 – 10 mins) it was slightly lower above this depth (~1.0 gL^{-1} at the water table), indicating very rapid dilution. Fairly uniform dilution occurred down to around 35 mbgl, with tracer concentrations approaching background in about 60 mins. Below these depths dilution was slower.

Figure 5 shows selected Pitrak et al. (2007) analyses for the above tests (NB Pitrak plots were prepared for all depths but only illustrative examples are shown here). Figure 5a and b show linear responses indicating horizontal crossflow in LKF at depths of 23.5 and 35 mbgl, with some vertical flow influence at the latter depth due to the relatively better fit at the former depth; Fig. 5c shows a non-linear response for depth 33.5 mgbl in WTP, indicating that vertical flows contribute to tracer loss at this depth.

5.1.2 Point injection tests

The results for point injection tests in TP, LKF and WTP boreholes are shown in Figures 6 and 7 (NB point injecting FHK borehole was not undertaken for logistical reasons). In TP borehole point injection test at depth 45 mbgl (Figure 6a(ii)), the injected tracer slug moved upwards to the area of enlarged diameter indicating upwards flow in the borehole, progressively losing tracer mass. [NB tracer mass for first profile (0-3 mins) of 81 g exceeded injected mass of 75 g, indicating incomplete mixing just after injection]. Note that no mass was lost between the second and third profiles, ie between depths 38 and 27.5 mbgl, indicating that tracer was conserved in the borehole between these depth.

For LKF point injection tests at depths 19.5 and 30 mbgl (monitoring discontinued after 31 min for 30 mbgl injection for logistical reasons) (Figure 6b (ii & iii)) respectively, the profiles show continuous mass loss with time but little vertical movement of the tracer slugs, confirming the dominance of lateral horizontal crossflows over vertical flows in the borehole as seen in the uniform injection test (Figure 4d).

Due to the complexity of flowing signatures from uniform injections in WTP borehole (Fig. 4c), three depths were point injected: 39.5, 33.5, and 41.5 mbgl (Figures 7c – e respectively). In the 39.5 m injection test (Figure 7c) tracer moves upwards to 34 mbgl progressively losing mass, with no tracer moving past this depth [the mass from the first profile (1-7 mins) of 84 g again exceeded the injected mass of 75 g, indicating incomplete mixing within the water column]. In the 33.5 m injection (Figure 7d), the tracer slug moves upwards towards the water table at 25 mbgl, progressively losing mass and velocity (most of the mass loss occurring immediately below the water table between 27.5 to 25 mbgl). In the 41.5 m injection (Figure 7e), profiles show little vertical movement of tracer with the peaks progressively reducing with time, indicating crossflow [mass from first profile (0-4 mins) of 43 g is in this case less than the 75 g injected].

5.2 Interpretation

5.2.1. Cases showing vertical flows

Interpretations of flow patterns for TP and WTP boreholes, which show vertical flows in some sections, are presented in Figure 8. Figure 8b and e show vertical flow velocities interpolated from the tracer slug centroid migration rates and tracer slug percentage masses remaining inferred from sequential profiles shown in Figures 6 and 7. Part c and f show conceptual models of inflows and out-flows from the boreholes, quantified by sequential application of Equation (7) to each velocity section, in consonance with caliper logs (Figure 8a and d).

For TP borehole (Figure 8c), depths 45 – 38 mbgl show inflow and crossflow, depth interval 38 – 19 mbgl mainly shows upflow, whereas depth interval 19 – 15 mbgl has outflow corresponding to a major interval of borehole enlargement. Little mass loss and fairly constant upwards velocity between depth 38 – 19 mbgl is suggestive of a zone without inflow or outflow (the small change in vertical velocity around between 27.5 mgbl and 19 mbgl may reflect diameter enlargement). The average upwards flow velocity in this current work of 2.1 m min^{-1} agrees with average impeller ambient upward flow speed of 2 m min^{-1} from 43 – 15 mbgl, as reported by Parker et al (2019) for TP borehole.

For WTP borehole (Figure 8f), the water in the borehole below ~42 m bgl is stagnant (see Fig 4c); above this depth to ~40 mbgl (kink in uniform injection profile Fig 4c) the borehole shows inflow and crossflow, depth interval 39 to 34 mbgl shows upflow with some outflow above 37 mbgl, while the 34 – 33m depth interval shows net inflow (evidenced by the increase upflow velocity above this, Fig 8e). Upflow velocity begins to fall above ~30m bgl and major tracer mass loss occurs in the depth interval 27.5 – 25 mbgl suggesting progressive outflow corresponding to the major interval of borehole enlargement immediately below the water table. In contrast Parker et al. (2019) used uniform single borehole injection test at a time of higher water table, to infer inflows at 40 m and 21 mbgl, with flow moving upwards and downwards respectively within the borehole to converge at an outflow between these depths (33.5 mbgl). Comparing the current flow WTP flow model with that from Parker et al (2019) suggests flow regimes can switch in response to seasonal water table variations {Parker et al

(2019) similarly measured larger magnitude borehole flow velocities above 33.5 mbgl than below as in this study, indicating the most active flow zone is above this depth}.

In summary, both the vertical flow cases represent boreholes in valley locations (TP and WTP boreholes, see Figure 1) showing developed permeability at depth with vertical hydraulic gradients that drive flow up the borehole, probably resulting from connection to recharge areas of higher hydraulic heads. The vertical flowrate in the outflow zone of TP is about 2 orders of magnitude higher than that from WTP probably indicates a larger head difference between intercepted flow horizons in TP.

5.2.2 Horizontal flow only case

Analysis of data from LKF borehole, which is an example that shows only horizontal cross flow, is presented in Figure 9. Pitrak et al. (2007) analysis as illustrated in Figure 5 for two selected depths have been applied to the responses at all depths to produce horizontal specific discharge across the borehole (q_w) at 1.5 m depth intervals (Figure 9b). The calculated discharges are highest within the zone of water table fluctuation in coincidence with the zone of enhanced diameter in the caliper logs (Figure 9a), reducing towards the bottom of the borehole, with a marked drop below 35 mbgl. The results are consistent with solutionally enlarged fractures near the water table, creating the zone of greatest permeability and flow. In this case, despite the valley location of the borehole, it does not seem to have intersected any permeability features with higher hydraulic head at depth, hence the lack of vertical flow in the borehole.

5.2.3 Inference of flowing porosities and groundwater velocities

In this section we explain how the flows detected in the boreholes using the single borehole dilution approach can potentially be used to infer flowing porosities and groundwater velocities in the aquifer In order to do this, it is necessary to have hydraulic test data relating to the overall borehole transmissivity as borehole as an indication of the number and distribution of flowing fractures e.g.

from a caliper log interpretation integrated with image and flow logs. In our study, transmissivity was only available for LKF borehole (8810 m^2/day) determined in a pumping test (Ward and Williams, 1995), hence, we only applied the workflow to this case. The transmissivity of each 1.5m section T_i (Figure 9c) was determined by assuming it was proportional to the specific discharge (Figure 9b) for that section. The number of fractures in each 1.5m section N_i is annotated on Figure 9c; note this reduces near the bottom of the borehole. T_i and N_i were then used to determine flowing porosity for each depth interval using equations 8 and 10. Using equation (9), individual fracture transmissivities ranged between 10 – 560 m^2/d (at the bottom and within the water table fluctuation zone respectively of the borehole. The flowing porosities (Figure 9d) range between 3.7×10^{-4} – 4.1×10^{-3} with an average of 2.1×10^{-3}, with highest values within the zone of water table fluctuation, coinciding with the largest caliper enlargements and the lowest values near the borehole base. The average porosity for this work is similar to the lower end of the range of pumping test-derived flowing porosities for Chalk reported by Foster and Milton (1974) and Ward and Williams (1995) as 5×10^{-3} – 1×10^{-1} and 3×10^{-3} – 2.2×10^{-2} respectively. In comparison with previous works, this current work also captured the lower porosity values below the depth of solutional features, whereas pumping tests from the previous works mainly characterise flowing features within the depth of water table fluctuation.

Theoretically, it is possible to use either equation (5) or equation (11) to determine groundwater velocities within the fractures once the flowing porosity is determined. However, the use of equation (5) requires a borehole convergence factor α to be assumed. Borehole convergence factors are often assumed to be 2 for granular aquifers (Freeze and Cherry, 1979) but are typically much larger for fractured aquifers, in some cases as high as 7 – 8 (Hall, 1993) or even > 10 (Kearl, 1997). Hence, we argue that use of equation (5) as previously used by Maldaner et al., (2018) introduces excessive uncertainty. Here, we instead use equation (11) which requires the horizontal hydraulic gradient in the aquifer, rather than the convergence factor. In using regional hydraulic gradient, we assume that groundwater velocities represent far-field velocities and also that the flowing zone is mostly relatively thin compared to the horizontal flow distances in the borehole-to-borehole tests, so vertical variations in hydraulic gradient may not be important in the analyses. An average hydraulic gradient of 3.3 x 10^{-3} was used based on historic hydraulic head measurements in the in study catchment (Ward and Williams, 1995). The inferred horizontal groundwater velocities from the single borehole test range between 60 – 850 md^{-1} (Figure 9e) with the higher values in the zone of enlarged flowing features in the upper parts of the borehole. These ‘single borehole-test’ horizontal groundwater velocities are similar i.e. bound within the upper (thick dashed lines) and lower limits of 50 – 480 md^{-1} respectively, as reported by Ward and William (1995) based on borehole-to-borehole tracer test groundwater velocities in the Kilham area (see Figure 1 for locations of these tests). There is excellent agreement between the single borehole-test velocities and borehole-to-borehole tracer tests within the water table fluctuation zone.

This level of agreement suggests that single borehole tests can provide accurate groundwater velocities despite their difference in scale of investigation from borehole-to-borehole tests (in this case the injection and detection points in the latter were up to 4.2 km apart). However, the results of the single-borehole analyses (both for flowing porosity and groundwater velocity) are sensitive to the identification of flowing fractures. Using caliper log enlargements overestimates the number of flowing features, since enlargements could represent drilling and flint layer effects rather than fractures. Secondly, ambient flow may be influenced by different fractures than those that contribute to transmissivity under pumped conditions Also, fractures within any given interval may have a wide range of hydraulic apertures rather than a single value as assumed in the use of the Cubic Law. Nevertheless, the single borehole approach provides a valuable additional low-cost tool for aquifer characterisation and delineation of groundwater velocities and hence borehole-head protection zones.

5.3 Discussion

The workflow and results obtained in this study have implications for characterisation, groundwater modelling, and resource management and protection of the specific aquifer investigated, i.e. the

Northern Province Chalk, and for similar limestone aquifers, but also for fractured and karstic aquifers generally. Firstly, preferential flow paths and vertical head gradients need consideration in the planning and interpretation of groundwater sampling and hydraulic head monitoring. Fast flows through some sections of the open-section boreholes tested, suggest that purging of such boreholes during sampling is not a prerequisite for this aquifer as water in these sections is not stagnated. Secondly, to obtain depth specific samples in boreholes, it would be appropriate to install multi-level piezometers or else apply straddle packers. However, it is appreciated that such works are expensive, so where open boreholes are sampled using bailers etc., as is still common practice, employment of borehole dilution tests beforehand allows appropriate depth selection and interpretation of which horizons are supplying the sampled water, allowing that seasonal changes may occur. For pumped samples to be representative of water from the whole borehole, the applied pumping rate needs should be sufficient (i.e. to exceed the likely borehole vertical flow rates) to sample the full range of flowing features. Furthermore, groundwater heads measured in open boreholes will represent transmissivity-weighted composite head in each of the individual horizons connected to the open borehole. Multi-level piezometers are needed to establish hydraulic head in each separate horizon, in order to characterise vertical hydraulic gradients. Use of multi-level piezometers installed at selected depths based on flow logging and potentially, dilution test data also has the advantage that open boreholes cannot themselves act as potential conduits for contaminants to enter groundwater, or influence the flow pattern in the aquifer overall.

This work has also shown the use of single borehole tests in conjunction with geophysical logs and hydraulic gradients external to the borehole for inferring borehole and aquifer scale properties. Firstly, for boreholes dominated by horizontal flows, the use of dilution tests to apportion interval transmissivity is a cheaper option compared to packer tests (Quinn et al., 2011; Maldaner et al., 2018), FLUTe profiling (Keller et al., 2013), piezometer installation (Medici et al., 2019) and flow logging (Molz et al., 1989; Parker et al., 2010). The transmissivity apportionment in this workflow although developed only for the horizontal flow case, has potential for further development and extension to vertical flow cases. Secondly, although the current work applies the theory of previous works, this is the first work to use single borehole dilution tests combined with long-interval pumping test data to rather than slug tests or packer profiling to depth-distribute flowing porosity. Thirdly, using the determined aquifer parameters for the horizontal flow case, we characterised groundwater velocities using externally measured hydraulic gradient which compared to other previous works avoided the assumptions of a flow convergence factor α and its inherent uncertainties. Our methodology for determining horizontal groundwater velocities has potential for widespread use on other fractured aquifers. Finally, although equation (7) has been theorized in other works, this work successfully implements it to infer inflow, outflow zones and vertical flow for the development and constraining of borehole scale conceptual models. Note that although we were not able to determine groundwater velocities from borehole tests showing vertical flow components because of the difficulty in distributing borehole transmissivity to individual features, the approach could be further developed for such cases where individual feature transmissivity measurements be available from e.g. packer tests. Finally, we note that the presence of open borehole sections within aquifers will modify their natural flow patterns, where these act as conduits for vertical flows. In relatively permeable systems such as the Chalk, open boreholes will add to natural flow pathways via vertical communicating features (faults, joints etc) but with overall small effect on the regional flow system. However, such effects may limit efficacy of the approach in lower permeability systems where such perturbations may influence regional flow.

In the study area, important discrete flow horizons are found throughout the tested depths.. Our data suggest that these flow features reduce in both frequency and permeability with depth possibly due to reduced fracture enlargement from slower groundwater circulation or other constrains on the development of flow features at particular level via karst genesis (Allen et al., 1997; Ford and Williams, 2007).. This is expected for the Chalk as seen in previous works (Williams et al., 2006; Maurice et al., 2010; Farrant et al., 2016; Parker et al., 2019). The vertical distribution of flow horizons in boreholes together with the dilution test results imply that the bulk of formation effective porosity and borehole transmissivity lies within the zone of water table fluctuation, indicating that resource assessment and valuation must be done in conjunction with a consideration for seasonality and using geophysical logs. The flow regime change observed in WTP borehole in response to seasonal hydraulic head variations is important not only for the Chalk, but other unconfined fractured aquifers with respect to contaminant monitoring and aquifer remediation.

The results of this work (low effective porosities, flow at discrete horizons, fast groundwater velocities) and previous tracer test results are typical of a karstic aquifer, implying that the Chalk is vulnerable to pollution as contaminants have short travel times from recharge areas to boreholes. The findings also have implication for conceptual solute transport model development for the purpose of well-head protection. Modelling aquifers such as Chalk with preferential flowpaths can be fraught with uncertainties. We recommend using a multiple conceptual model approach and systematically collecting data to test and constrain transport models (Brassington and Younger, 2010; Worthington, 2015; Bredehoeft, 2005). In this type of aquifer, it is essential that models purporting to simulate both available resource and solute transport correctly incorporate seasonality, given the dominant nature of the (often rather thin) zone of solutionally enhanced permeability in the zone of water table fluctuation.

The implementation of our workflow shows the potential for open-borehole dilution tests in reducing costs of hydrogeological investigations at both the borehole and catchment scale, for aquifer characterisation, prediction of horizontal groundwater velocities and development of sound conceptual models. This relatively cheap workflow is potentially applicable for the characterisation of other fractured aquifers.

6. Conclusion

Knowledge of preferential flowpaths and vertical head gradients are important for characterising groundwater in fractured aquifers like the Cretaceous Chalk. However, because of their heterogenous and anisotropic nature, detailed characterisation of such aquifers is needed for adequate modelling of both resource and pollution vulnerability. Borehole-to-borehole 'catchment' scale tracer tests are one effective way of characterising such aquifers but are time consuming and expensive to perform. Single borehole dilution tests are cheaper to perform, their results have previously been considered more difficult to interpret. In this study, we propose a new workflow for ambient flow single borehole dilution tests showing that where interpreted in conjunction with other data, they can be effectively used to characterise and constrain flowing features in fractured and karstic aquifers, and that their results are consistent with those from other more expensive approaches.

In the study reported here of the unconfined Cretaceous Chalk aquifer of East Yorkshire, UK, single borehole dilution tests were used to identify flowing features in monitoring boreholes with long open sections, from the dilution pattern shown by the injected tracer due to inflowing formation water under natural (ambient) flow conditions. Both uniform injection (tracer distributed over whole section of the borehole that is open to the aquifer) and point injection tracer test (discrete slug of tracer injected at a single depth) were performed. The tracer tests were initially qualitatively interpreted via signature methods to distinguish between boreholes dominated by vertical and horizontal flows. Then, for the case of boreholes dominated by horizontal flow, test data were interpreted in combination with long-interval pumping test data transmissivity and geophysical logs to yield fracture kinematic porosity versus depth. Flowing porosities ranged between $3.7 \times 10^{-4} – 4.1 \times 10^{-3}$, in good agreement with those found using other methods. Combining with external hydraulic gradient, these data yielded depth distributed horizontal groundwater velocities of 60 – 850 md^{-1}, which closely agreed with those from borehole-to-borehole tracer tests (50 – 480 md^{-1}) reported in previous studies of the same catchment. [Note that the use of external hydraulic gradients for the derivation of horizontal groundwater velocities proposed here circumvents many uncertainties associated with previous interpretational approaches for single borehole data.] For boreholes showing vertical flow, both uniform and point injection tracer test data were interpreted in conjunction with geophysical logs to yield in-borehole vertical flow velocities, and hence characterise borehole inflows, crossflows and outflows. Vertical velocities inferred from the borehole dilution tests broadly agreed with those measured using flow logging tests conducted in previous work in the same boreholes. The identified flowing features were used to infer conceptual flow models, enabling an improved understanding of catchment-scale aquifer heterogeneities.

The findings from this work show that long-interval single borehole dilution tests represent a low cost but effective hydrogeological tool for the characterisation of fractured and karstic aquifers. They can be employed on open boreholes in consolidated fractured aquifers in order to target depths for sampling, further hydraulic testing, or piezometer installation. Combining uniform and point injection approaches allows verification of the interpretational approaches applied; point injection tests are particularly relevant where vertical flows occur within boreholes. For horizontal flow conditions, dilution test data can be used to distribute transmissivity from long-interval hydraulic tests, characterise fracture aperture and porosity, and in combination with externally-measured hydraulic gradients to infer groundwater velocities in the formation.

Acknowledgements

We thank Kirk Handley from the School of Earth and Environment for assisting in fieldwork. We also thank Dr Louise Maurice of the British Geological Survey for field kit support and guidance, and Rolf Farrell and Edward Wrathmell from the Environment Agency of England and Wales for input at the early stages of this work. We also thank two anonymous reviewers for their review comments.

Funding information

This work was made possible by: Scholarship Award No. GHCS – 2015- 147 from the joint sponsorship of the Commonwealth Scholarship Commission (CSC) UK and University of Leeds; Fieldwork Support Grant and data licensing from the UK Environment Agency.

References

Akoachere, R.A.I.I. and Van Tonder, G. 2009. Two new methods for the determination of hydraulic fracture apertures in fractured-rock aquifers. *Water SA*. **35**(3),pp.349–360.

Allen, D.J., Brewerton, L.J., Coleby, L.M., Gibbs, B.R., Lewis, M.A., MacDonald, A.M., Wagstaff, S.J. and Williams, A.T. 1997. *The physical properties of major aquifers in England and Wales.British Geological Survey Technical Report WD/97/34.Environment Agency R&D Publication 8*. British Geological Survey Technical Report WD/97/34.

Bloomfield, J. 1996. Characterisation of hydrogeologically significant fracture distributions in the Chalk: An example from the Upper Chalk of southern England. *Journal of Hydrology*. **184**(3–4),pp.355–379.

Bottrell, S.H., Thornton, S.F., Spence, M.J., Allshorn, S. and Spence, K.H. 2010. Assessment of the use of fluorescent tracers in a contaminated Chalk aquifer. *Quarterly Journal of Engineering Geology and Hydrogeology*. **43**(2),pp.195–206.

Boulding, J. 1993. *Subsurface Characterization and Monitoring Techniques. A Desk Reference Guide. Volume I: Solids and Ground Water Appendices A and B. EPA/625/R-93/003a*. Washington, DC.

Brainerd, R.J. and Robbins, G.A. 2004. A tracer dilution method for fracture characterization in bedrock wells. *Ground water*. **42**(5),pp.774–780.

Brassington, F.C. 1992. Measurements of Head Variations within Observation Boreholes and their Implications for Groundwater Monitoring. *Water and Environment Journal*. **6**(3),pp.91–100.

Brassington, F.C. and Younger, P.L. 2010. A proposed framework for hydrogeological conceptual modelling. *Water and Environment Journal*. **24**(4),pp.261–273.

Bredehoeft, J. 2005. The conceptualization model problem — surprise. *Hydrogeology Journal*. **13**,pp.37–46.

Buckley, D.K. and Talbot, J.C. 1994. *Interpretation of geophysical logs of the Kilham area, Yorkshire Wolds, to support groundwater tracer studies*. British Geological Survey Technical

Report,WD/94/10C.

Cook, P.G. 2003. *A guide to regional groundwater flow in fractured rock aquifers*. South Australia: CSIROSeaview Press.

Dalton, M.G., Huntsman, B.E. and Bradbury, K. 2006. Acquisition and interpretation of water level data *In*: D. Nielsen and G. L. Nielsen, eds. *The essential handbook of ground-water sampling*. Boca Raton, Florida: CRC Press, p. 309.

Datel, J. V., Kobr, M. and Prochazka, M. 2009. Well logging methods in groundwater surveys of complicated aquifer systems: Bohemian Cretaceous Basin. *Environmental Geology*. **57**(5),pp.1021–1034.

Day-Lewis, F.D., Johnson, C.D., Paillet, F.L. and Halford, K.J. 2011. A Computer Program for Flow-Log Analysis of Single Holes (FLASH). *Ground Water*. **49**(6),pp.926–931.

Doughty, C., Takeuchi, S., Amano, K., Shimo, M. and Tsang, C.-F. 2005. Application of multirate flowing fluid electric conductivity logging method to well DH-2, Tono Site, Japan. *Water Resources Research*. **41**(10),pp.1–16.

Doughty, C., Tsang, C.-F., Hatanaka, K., Yabuuchi, S. and Kurikami, H. 2008. Application of direct-fitting, mass integral, and multirate methods to analysis of flowing fluid electric conductivity logs from Horonobe, Japan. *Water Resources Research*. **44**(8),pp.1–19.

Doughty, C. and Tsang, C. 2005. Signatures in flowing fluid electric conductivity logs. *Journal of Hydrology*. **310**,pp.157–180.

Downing, R.A. 1998. *Groundwater - our hidden asset*. Produced by the UK Groundwater Forum. Published by the British Geological Survey.

Drost, W., Klotz, D., Koch, A., Moser, H., Neumaier, F. and Rauert, W. 1968. Point dilution methods of investigating ground water flow by means of radioisotopes. *Water Resources Research*.

4(1),pp.125–146.

Edmunds, W.M., Buckley, D.K., Darling, W.G., Milne, C.J., Smedley, P.L. and Williams, A.T. 2001. Palaeowaters in the aquifers of the coastal regions of southern and eastern England. *Geological Society, London, Special Publications*. **189**(1),pp.71–92.

Farrant, A.R., Woods, M.A., Maurice, L., Haslam, R., Raines, M. and Kendall, R. 2016. *Geology of the Kilham area and its influence on groundwater flow. British Geological Survey Commissioned Report CR/16/023*.

Ford, D. and Williams, P. 2007. *Karst Hydrogeology and Geomorphology*. Chichester: Wiley.

Foster, S.S.D. and Milton, V.A. 1976. *Hydrogeological basis for large-scale development of groundwater storage capacity in the East Yorkshire Chalk.* Report of the Institute of Geological Sciences, 76/7.

Foster, S.S.D. and Milton, V.A. 1974. The permeability and storage of an unconfined chalk aquifer. *Hydrological Sciences Bulletin*. **XIX**(4),pp.485–500.

Freeze, R.A. and Witherspoon, P.A. 1968. Theoretical Analysis of Regional Ground Water Flow 3. Quantitive Interpretions. *Water Resources Research*. **4**(3),pp.581–590.

Gale, I.N. and Rutter, H.K. 2006. *The Chalk aquifer of Yorkshire*. British Geological Survey Research Report. RR/06/04.

Gustafsson, E. and Anderson, P. 1991. Groundwater flow conditions in a low-angle fracture zone at Finnsjon, Sweden. *Journal of Hydrology*. **126**,pp.79–111.

Hall, S.H. 1993. Single Well Tracer Tests in Aquifer Characterization. *Groundwater Monitoring & Remediation*. **13**(2),pp.118–124.

Jones, H., Gale, I., Barker, J. and Shearer, T. 1993. *Hydrogeological report on the test pumping of Hutton Cranswick, Kilham, and Elmswell boreholes. British Geological Survey Technical Report,* *WD/93/9.*

Kearl, P. 1997. Observations of particle movement in a monitoring well using the colloidal borescope. *Journal of Hydrology*. **200**,pp.323–344.

Keller, C.E., Cherry, J.A. and Parker, B.L. 2013. New method for continuous transmissivity profiling in fractured rock. *Groundwater*. **52**(3),pp.352–367.

Keys, W.S. 1990. *Chapter E2. Borehole geophysics applied to ground-water investigations. Techniques of Water-Resources Investigations of the United States Geological Survey*. United States Geological Survey.

Knapp, M.F. 2005. Diffuse pollution threats to groundwater: A UK water company perspective. *Quarterly Journal of Engineering Geology and Hydrogeology*. **38**(1),pp.39–51.

Kobr, M. 2003. Geophysical techniques applied to aquifer hydrodynamics. *Bollettino di Geofisica Teorica ed Applicata*. **44**(3–4),pp.307–319.

Lewis, D.C., Kriz, G.J. and Burgy, R.H. 1966. Tracer dilution sampling technique to determine hydraulic conductivity of fractured rock. *Water Resources Research*. **2**(3),pp.533–542.

Liang, X., Liu, Y., Jin, M., Lu, X. and Zhang, R. 2010. Direct observation of complex Tothian groundwater flow systems in the laboratory. *Hydrological Processes*. **3573**,pp.3568–3573.

Maldaner, C.H., Quinn, P.M., Cherry, J.A. and Parker, B.L. 2018. Improving estimates of groundwater velocity in a fractured rock borehole using hydraulic and tracer dilution methods. *Journal of Contaminant Hydrology*. [Online]. **214**(May),pp.75–86. Available from: https://doi.org/10.1016/j.jconhyd.2018.05.003.

Maurice, L., Barker, J.A., Atkinson, T.C., Williams, A.T. and Smart, P.L. 2010. A Tracer Methodology for Identifying Ambient Flows in Boreholes. *Ground Water*. **49**(2),pp.227–238.

McMillan, L.A., Rivett, M.O., Tellam, J.H., Dumble, P. and Sharp, H. 2014. Influence of vertical flows in wells on groundwater sampling. *Journal of Contaminant Hydrology*. [Online]. **169**,pp.50–61. Available from: http://dx.doi.org/10.1016/j.jconhyd.2014.05.005.

Medici, G., West, L. and Banwart, S. 2019. Groundwater flow velocities in a fractured carbonate aquifer-type : Implications for contaminant transport. *Journal of Contaminant Hydrology*. [Online]. **222**,pp.1–16. Available from: https://doi.org/10.1016/j.jconhyd.2019.02.001.

Moir, R.S., Parker, A.H. and Bown, R.T. 2014. A simple inverse method for the interpretation of pumped flowing fluid electrical conductivity logs. *Water Resources Research*. (50),pp.6466–6478.

Molz, F.J., Morin, R.H., A.E., H., Melville, J.G. and Guven, O. 1989. The Impeller Meter for Measuring Aquifer Permeability Variations: Evaluation and Comparison with Other Tests. *Water Resources Research*. **25**(7),pp.1677–1683.

Novakowski, K., Bickerton, G., Lapcevic, P., Voralek, J. and Ross, N. 2006. Measurements of groundwater velocity in discrete rock fractures. *Journal of Contaminant Hydrology*. **82**(1–2),pp.44–60.

Novakowski, K.S., Lapcevic, P.A., Voralek, J. and Bickerton, G. 1995. Preliminary interpretation of tracer experiments conducted in a discrete rock fracture under condition of natural flow. *Geophysical Research Letters*. **22**(11),pp.1417–1420.

Paillet, F.L. 1991. Use of geophysical well logs in evaluating crystalline rocks for siting of radioactive waste repositories. *The Log Analysit*. **32**(2),pp.85–107.

Paillet, F.L. and Pedler, W.H. 1996. Integrated borehole logging methods for wellhead protection applications. *Engineering Geology*. **42**(2–3),pp.155–165.

Paillet, F.L., Williams, J.H., Urik, J., Lukes, J., Kobr, M. and Mares, S. 2012. Cross-borehole flow analysis to characterize fracture connections in the Melechov Granite, Bohemian-Moravian Highland, Czech Republic. *Hydrogeology Journal*. **20**(1),pp.143–154.

Parker, A.H., West, L.J. and Odling, N.E. 2019. Well flow and dilution measurements for characterization of vertical hydraulic conductivity structure of a carbonate aquifer. *Quarterly Journal of Engineering Geology and Hydrogeology*. [Online]. **52**(1),pp.74–82. Available from: https://doi.org/10.1144/qjegh2016-145.

Parker, A.H., West, L.J., Odling, N.E. and Bown, R.T. 2010. A forward modeling approach for interpreting impeller flow logs. *Ground Water*. **48**(1),pp.79–91.

Pedler, W.H., Barvenik, C.F., Tsang, C.F. and Hale, F.V. 1990. Determination of Bedrock Hydraulic Conductivity and Hydrochemistry Using a Wellbore Fluid Logging Method *In*: *Proceedings of the Fourth National Outdoor Action Conference on Aquifer Restoration,Ground Water Monitoring and Geophysical Methods, Las Vegas,Nevada, Dublin,Ohio:National Well Water Association*., pp. 39–53.

Pedler, W.H., Head, C.L. and Williams, L.H. 1992. Hydrophysical Logging: A New Wellbore Technology for Hydrogeologic and Contaminant Characterization of Aquifers *In*: *Proceedings of the Sixth National Outdoor Action Conference on Aquifer Restoration,Ground Water Monitoring and Geophysical Methods, Las Vegas,Nevada, Dublin,Ohio:National Well Water Association*., pp. 701–715.

Piccinini, L., Fabbri, P. and Pola, M. 2016. Point dilution tests to calculate groundwater velocity: an example in a porous aquifer in northeast Italy. *Hydrological Sciences Journal*. [Online]. **61**(8),pp.1512–1523. Available from: http://dx.doi.org/10.1080/02626667.2015.1036756.

Pitrak, M., Mares, S. and Kobr, M. 2007. A simple borehole dilution technique in measuring horizontal ground water flow. *Ground Water*. **45**(1),pp.89–92.

Price, M. 1987. Fluid flow in the Chalk of England *In*: J. C. Goff and B. P. J. Williams, eds. *FluidFlow in Sedimentary Basins and Aquifers*. Geological Society Special Publication, pp. 141–156.

Price, M., Low, R.G. and McCann, C. 2000. Mechanisms of water storage and flow in the unsaturated zone of the Chalk aquifer. *Journal of Hydrology*. **233**(1–4),pp.54–71.

Qian, J., Chen, Z., Zhan, H. and Guan, H. 2011. Experimental study of the effect of roughness and Reynolds number on fluid flow in rough-walled single fractures : a check of local cubic law. *Hdyrological Processes*. **622**,pp.614–622.

Quinn, P.M., Parker, B.L. and Cherry, J.A. 2011. Using constant head step tests to determine hydraulic apertures in fractured rock. *Journal of Contaminant Hydrology*. **126**(1–2),pp.85–99.

Saines, M. 1981. Errors in the interpretation of groundwater level data. *Groundwater Monitoring and Remediation, Spring Issue*.,pp.56–51.

Shuter, E. and Teasdale, W.E. 1989. *Application of Drilling, Coring and Sampling Techniques to Test Holes and Wells. Techniques of Water-Resource Investigations of the United States Geological Survey. Book 2. Ch. F1*.

Singhal, B.B.S. and Gupta, R.P. 1999. *Applied Hydrogeology of Fractured Rocks*. Boston: Kluwer Academic Publishers.

Smedley, P., Neumann, I. and Farrell, R. 2004. *Baseline Report Series: 10. The Chalk Aquifer of Yorkshire and North Humberside.* British Geological Survey and UK Environment Agency.

Snow, D.T. 1969. Anisotropic Permeability of Fractured Media. *Water Resources Research*. **5**(6),pp.1273–1288.

van Tonder, G., Riemann, K. and Dennis, I. 2002. Interpretation of single-well tracer tests using fractional-flow dimensions. Part 1: Theory and mathematical models. *Hydrogeology Journal*. **10**,pp.351–356.

Toth, J. 1962. A Theory of Groundwater Motion in Small Drainage Basins Hydrology in Central Alberta, Canada. *Journal of Geophysical Research*. **67**(11),pp.4375–4387.

Toth, J. 2009. *Gravitational Systems of Groundwater Flow: Theory, Evaluation, Utilization*.

Cambridge: Cambridge University Press.

Tsang, C.-F. and Doughty, C. 2003. Multirate flowing fluid electric conductivity logging method. *Water Resources Research*. **39**(12),p.SBH 12-1-8.

Tsang, C., Hufschmied, P. and Hale, F.V. 1990. Determination of Fracture Inflow Parameters With a Borehole Fluid Conductivity Logging Method. *Water Resources Research*. **26**(4),pp.561–578.

Ward, R., Fletcher, S., Ever, S. and Chadha, S. 2000. Tracer testing as an aid to groundwater protection *In*: *Tracers and Modelling in Hydrogeology*. Liege, Belgium: IAH, pp. 85–90.

Ward, R., Williams, A., Barker, J., Brewerton, L. and Gale, I. 1998. *Groundwater Tracer Tests : a review and guidelines for their use in British aquifers*. British Geological Survey Technical Report, WD/98/19,Environment Agency R&D Technical Report W160.

Ward, R.S., Chadha, D.S., Aldrick, J. and Brewerton, L.J. 1998. *A Tracer Investigation of Groundwater Protection Zones around Kilham PWS Well, East Yorkshire. British Geological Survey Report WE/98/19*.

Ward, R.S. and Williams, A.T. 1995. *A tracer test in the Chalk near Kilham, North Yorkshire. British Geological Survey Report WD/95/7*.

Waters, A. and Banks, D. 1997. The chalk as a karstified aquifer: closed circuit television images of macrobiota. *Quarterly Journal of Engineering Geology*. **30**,pp.143–146.

Weight, W.D. 2008. *Hydrogeology Field manual* 2nd ed. New York: Mc-Graw Hill.

West, L.J. and Odling, N.E. 2007. Characterization of a multilayer aquifer using open well dilution tests. *Ground Water*. **45**(1),pp.74–84.

Williams, A., Bloomfield, J., Griffiths, K. and Butler, A. 2006. Characterising the vertical variations in hydraulic conductivity within the Chalk aquifer. *Journal of Hydrology*. **330**(1–2),pp.53–62.

Witherspoon, P.A., Wang, J.S.Y., Iwai, K. and Gale, J.E. 1980. Validity of Cubic Law for Fluid Flow in a

Deformable Rock Fracture. *Water Resources Research*. **16**(6),pp.1016–1024.

Worthington, S.R.H. 2015. Diagnostic tests for conceptualizing transport in bedrock aquifers. *Journal of Hydrology*. [Online]. **529**,pp.365–372. Available from: http://dx.doi.org/10.1016/j.jhydrol.2015.08.002.

Xu, Y., van Tonder, G.J., van Wyk, B., van Wyk, E. and Aleobua, B. 1997. Borehole dilution experiment in a Karoo aquifer in Bloemfontein. *Water SA*. **23**(2),pp.141–145.

Zemanek, J.O.E., Gleen, E.E., Norton, L.J. and Caldwell, R.L. 1970. Formation Evaluation by Inspection with the Borehole Televiewer. *Geophysics*. **35**(2),pp.254–269.

Paper figure labels

Figure 1: Study area: (a) Inset map of Great Britain and location of study area; (b) Single-borehole dilution test boreholes (red squares) with their elevation above ordnance datum superimposed on geology of study area, LKF BH: Little Kilham Farm Borehole, 39.96 mAoD; TP BH:Tancred Pit Borehole, 36.40 mAoD; FHK BH: Field House Farm, Kilham Borehole, 94.42 mAoD; WTP: Weaverthorpe Borehole, 70.00 mAoD. Black circles and arrows for borehole-to-borehole connectivity and resultant groundwater velocities between boreholes (HPT BH: Henpit Hole Borehole, 48.86 mAoD; MD BH: Middledale Borehole, 43.72 mAoD; LKF). © Crown Copyright & Database Right 2019. Ordnance Survey (Digimap Licence). Geological Map Data BGS © UKRI 2019.

Figure 2: Experimental set up: (a) Uniform open-borehole dilution test; (b) Point injection test.

Figure 3: Work flow and decision tree for analysing single-borehole dilution tests.

Figure 4: Example single borehole uniform test results: (a) FHK caliper and uniform injection (09/08/2017); (b) WTP borehole image log, caliper (Butcher and Townsend, 2017) and uniform injection (03/08/2017); (c) TP caliper and uniform injection (13/05/2016); (d) LKF caliper and uniform injection (20/07/2017).

Figure 5: Horizontal flow model regression plot for: (a) LKF depth 23.5 mbgl; (b) LKF depth 35 mbgl; (c) WTP depth 33.5 mbgl. Note axes scales vary.

Figure 6: TP (28/06/2016) and LKF (24/11/2017) single borehole point dilution test: (a) TP caliper and injection results for depth 45 mbgl; (b) LKF caliper log and injection results for depth: (ii) 19.5 mbgl; (iii) 30 mbgl.

Figure 7: WTP single borehole point injection test results (24/11/2017) (red arrows indicate depth of injection). (a) borehole optical image log (red dashed lines mark probable flowing features); (b) caliper log; (c), (d), (e) at: (c) 39.5; 33.5; and 41.5 mbgl respectively. (NB: The salinity peak in the bottom section of WTP is the remnant of NaCl left from the previous uniform injection test).

Figure 8: Vertical flow cases interpretation. (a) TP caliper log; (b) TP vertical velocity and mass plot (red dashed line) with depth (75 g injection depth 45 m bgl); (c) TP flow model; (d) WTP caliper log; (e) WTP velocity and mass plot (red dashed lines) with depth (75 g injection at depths 39.5 and 33.5 mbgl; (f) WTP flow model.

Figure 9: Interpretation for LKF HP horizontal flow case: (a) caliper log; (b) specific discharge in borehole, q_w with depth; (c) dilution apportioned transmissivity (T_i), with annotations of number of flowing features (N_i) inferred from caliper diameter enlargements in each 1.5 m depth interval (d) porosity variation with depth from cubic law; (e) horizontal groundwater velocities versus depth from single borehole tests compared with upper and lower limits from borehole-to-borehole tracer tests indicated in Figure 1 (dashed lines).

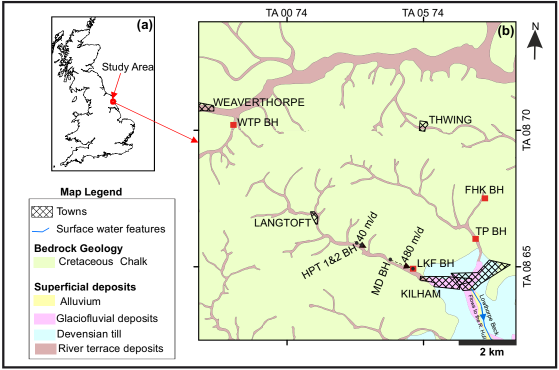

(a)
Study Area
(b)
TA 00 74
TA 05 74
N
WEAVERTHORPE
WTP BH
THWING
TA 08 70
FHK BH
LANGTOFT
40 m/d
TP BH
480 m/d
HPT 1&2 BH
MD BH
LKF BH
TA 08 65
KILHAM
Lowthorpe Beck
Flows to the R. Hull
2 km
Map Legend
Towns
Surface water features
Bedrock Geology
Cretaceous Chalk
Superficial deposits
Alluvium
Glaciofluvial deposits
Devensian till
River terrace deposits

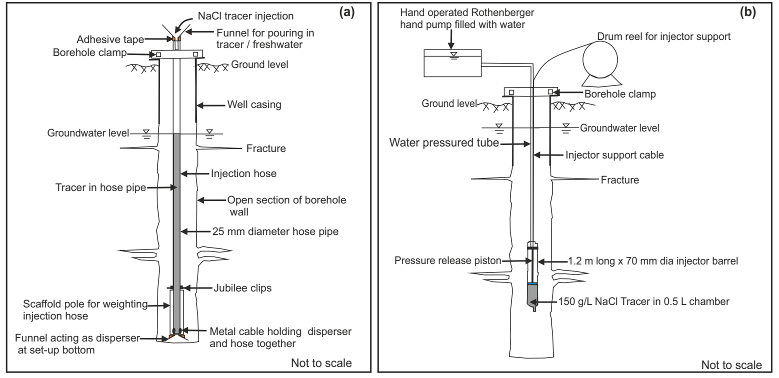
(a)
NaCl tracer injection
Adhesive tape
Funnel for pouring in tracer / freshwater
Borehole clamp
Ground level
Well casing
Groundwater level
Fracture
Injection hose
Tracer in hose pipe
Open section of borehole wall
25 mm diameter hose pipe
Jubilee clips
Scaffold pole for weighting injection hose
Funnel acting as disperser at set-up bottom
Metal cable holding disperser and hose together
Not to scale
(b)
Hand operated Rothenberger hand pump filled with water
Drum reel for injector support
Borehole clamp
Ground level
Groundwater level
Water pressured tube
Injector support cable
Fracture
Pressure release piston
1.2 m long x 70 mm dia injector barrel
150 g/L NaCl Tracer in 0.5 L chamber
Not to scale

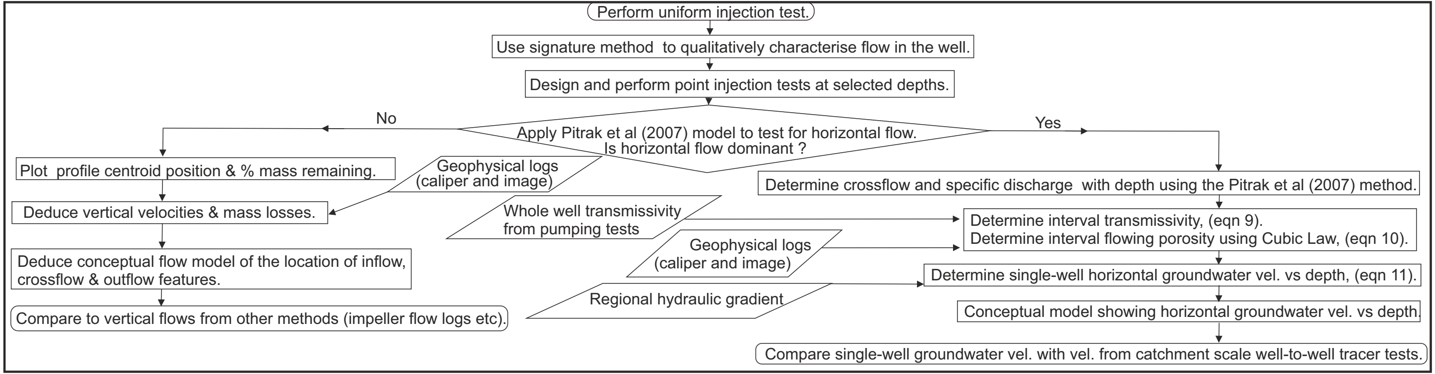

Perform uniform injection test.
Use signature method to qualitatively characterise flow in the well.
Design and perform point injection tests at selected depths.
No
Apply Pitrak et al (2007) model to test for horizontal flow.
Is horizontal flow dominant ?
Yes
Plot profile centroid position & % mass remaining.
Geophysical logs (caliper and image)
Deduce vertical velocities & mass losses.
Deduce conceptual flow model of the location of inflow, crossflow & outflow features.
Compare to vertical flows from other methods (impeller flow logs etc).
Determine crossflow and specific discharge with depth using the Pitrak et al (2007) method.
Whole well transmissivity from pumping tests
Determine interval transmissivity, (eqn 9).
Determine interval flowing porosity using Cubic Law, (eqn 10).
Geophysical logs (caliper and image)
Determine single-well horizontal groundwater vel. vs depth, (eqn 11).
Regional hydraulic gradient
Conceptual model showing horizontal groundwater vel. vs depth.
Compare single-well groundwater vel. with vel. from catchment scale well-to-well tracer tests.

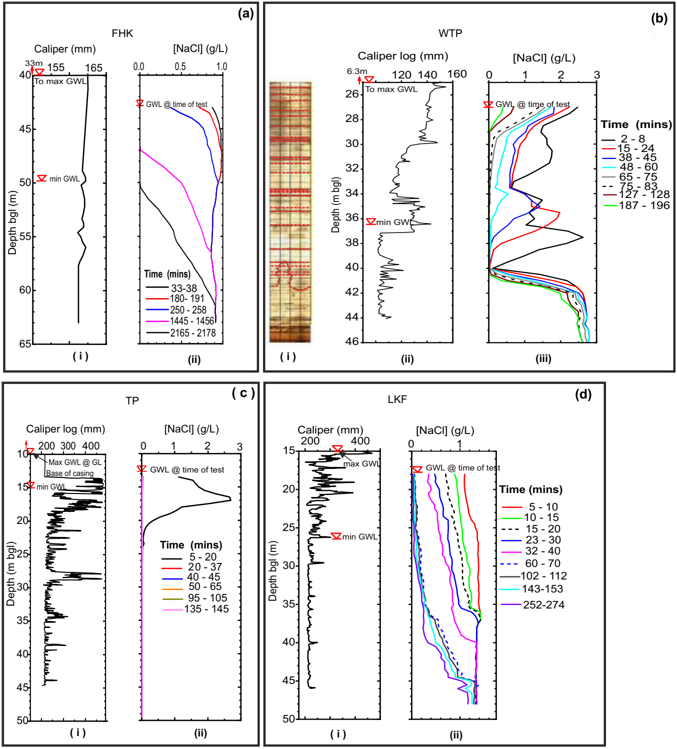

(a)
FHK
Caliper (mm)
[NaCl] (g/L)
33m
155
165
To max GWL
min GWL
Depth bgl (m)
GWL @ time of test
Time (mins)
33-38
180- 191
250 - 258
1445 - 1456
2165 - 2178
(i)
(ii)
(b)
WTP
Caliper log (mm)
6.3m
120
140
160
To max GWL
min GWL
Depth (m bgl)
GWL @ time of test
Time (mins)
2 - 8
15 - 24
38 - 45
48 - 60
65 - 75
75 - 83
127 - 128
187 - 196
(i)
(ii)
(iii)
(c)
TP
Caliper log (mm)
200
300
400
Max GWL @ GL
Base of casing
min GWL
Depth (m bgl)
GWL @ time of test
Time (mins)
5 - 20
20 - 37
40 - 45
50 - 65
95 - 105
135 - 145
(i)
(ii)
(d)
LKF
Caliper (mm)
200
400
max GWL
min GWL
Depth bgl (m)
GWL @ time of test
Time (mins)
5 - 10
10 - 15
15 - 20
23 - 30
32 - 40
60 - 70
102 - 112
143-153
252-274
(i)
(ii)

(a)

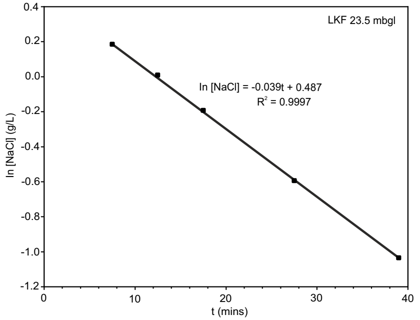
LKF 23.5 mbgl
ln [NaCl] = -0.039t + 0.487
R^2 = 0.9997
ln [NaCl] (g/L)
t (mins)
0.4
0.2
0.0
-0.2
-0.4
-0.6
-0.8
-1.0
-1.2
0
10
20
30
40

(b)

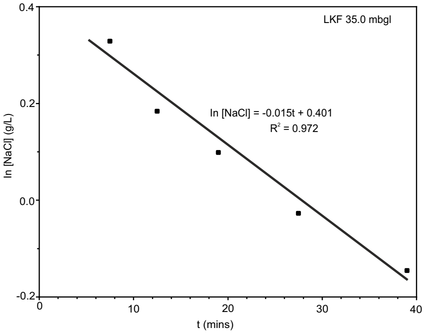
LKF 35.0 mbgl
ln [NaCl] = -0.015t + 0.401
R^2 = 0.972
ln [NaCl] (g/L)
t (mins)
0.4
0.2
0.0
-0.2
0
10
20
30
40

(c)

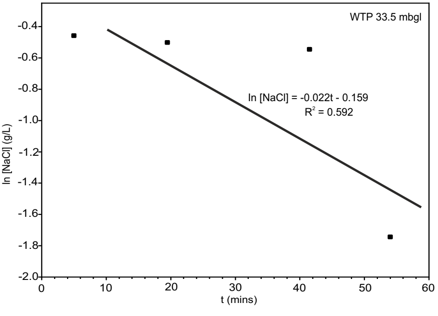
WTP 33.5 mbgl
ln [NaCl] = -0.022t - 0.159
R^2 = 0.592
ln [NaCl] (g/L)
t (mins)
-0.4
-0.6
-0.8
-1.0
-1.2
-1.4
-1.6
-1.8
-2.0
0
10
20
30
40
50
60

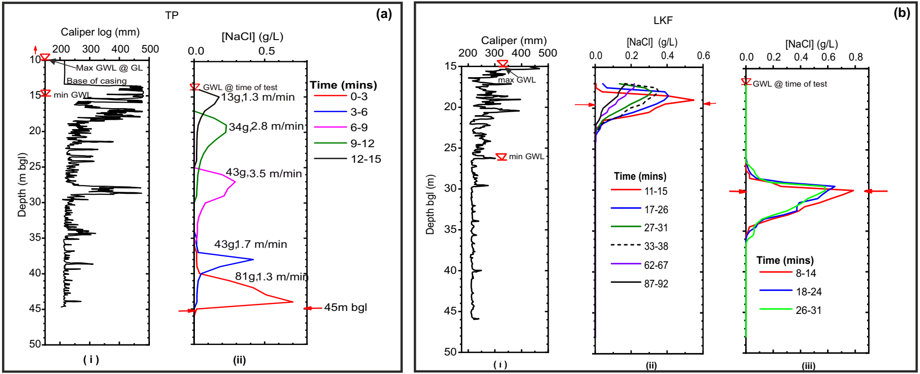

TP
(a)
Caliper log (mm)
200 300 400 500
Max GWL @ GL
Base of casing
min GWL
Depth (m bgl)
[NaCl] (g/L)
0.0 0.5
GWL @ time of test
13g,1.3 m/min
34g,2.8 m/min
43g,3.5 m/min
43g1.7 m/min
81g,1.3 m/min
45m bgl
Time (mins)
0-3
3-6
6-9
9-12
12-15
(i)
(ii)
LKF
(b)
Caliper (mm)
max GWL
min GWL
Depth bgl (m)
[NaCl] (g/L)
GWL @ time of test
Time (mins)
11-15
17-26
27-31
33-38
62-67
87-92
Time (mins)
8-14
18-24
26-31
(i)
(ii)
(iii)

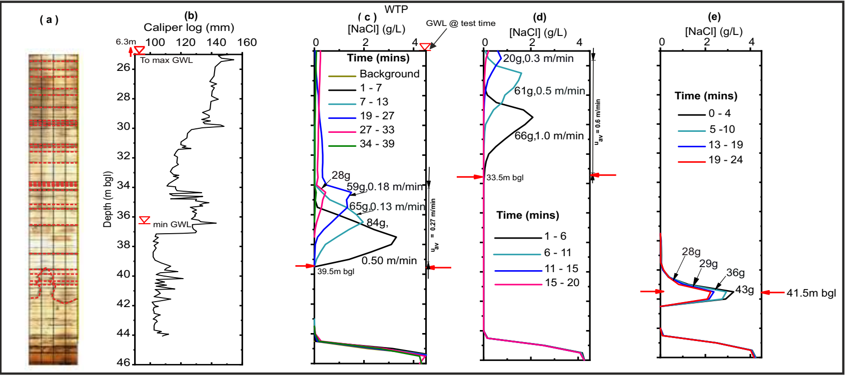

(a)
(b)
Caliper log (mm)
6.3m
100 120 140 160
To max GWL
min GWL
Depth (m bgl)
26 28 30 32 34 36 38 40 42 44 46
WTP
(c)
[NaCl] (g/L)
GWL @ test time
0 2 4
Time (mins)
Background
1 - 7
7 - 13
19 - 27
27 - 33
34 - 39
28g
59g,0.18 m/min
65g,0.13 m/min
84g,
0.50 m/min
39.5m bgl
u_av = 0.27 m/min
(d)
[NaCl] (g/L)
20g,0.3 m/min
61g,0.5 m/min
66g,1.0 m/min
u_av = 0.6 m/min
33.5m bgl
Time (mins)
1 - 6
6 - 11
11 - 15
15 - 20
(e)
[NaCl] (g/L)
Time (mins)
0 - 4
5 -10
13 - 19
19 - 24
28g
29g
36g
43g
41.5m bgl

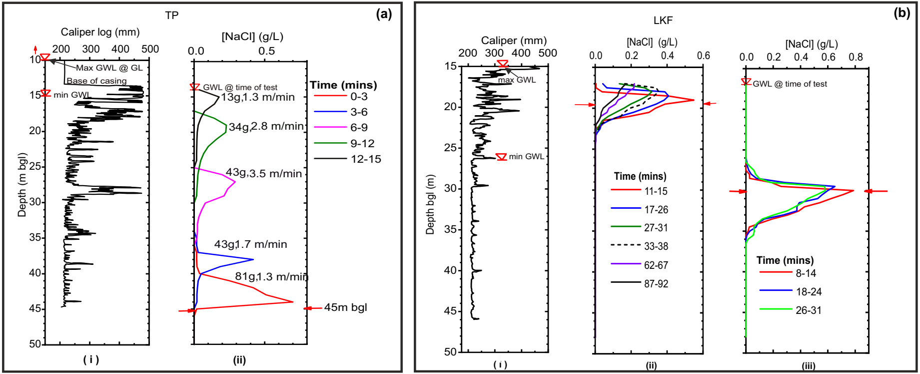

TP
(a)
Caliper log (mm)
[NaCl] (g/L)
Max GWL @ GL
Base of casing
min GWL
GWL @ time of test
13g,1.3 m/min
34g,2.8 m/min
43g,3.5 m/min
43g,1.7 m/min
81g,1.3 m/min
45m bgl
Time (mins)
0-3
3-6
6-9
9-12
12-15
Depth (m bgl)
(i)
(ii)
LKF
(b)
Caliper (mm)
max GWL
min GWL
[NaCl] (g/L)
Time (mins)
11-15
17-26
27-31
33-38
62-67
87-92
GWL @ time of test
Time (mins)
8-14
18-24
26-31
Depth bgl (m)
(i)
(ii)
(iii)

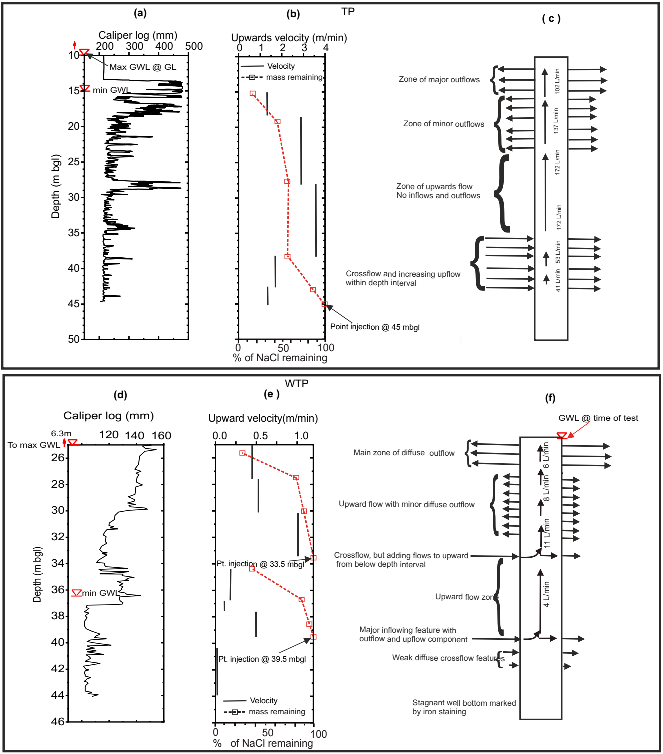

TP
(a)
Caliper log (mm)
200 300 400 500
Max GWL @ GL
min GWL
Depth (m bgl)
(b)
Upwards velocity (m/min)
0 1 2 3 4
Velocity
mass remaining
Point injection @ 45 mbgl
0 50 100
% of NaCl remaining
(c)
Zone of major outflows
Zone of minor outflows
Zone of upwards flow
No inflows and outflows
Crossflow and increasing upflow
within depth interval
102 L/min
137 L/min
172 L/min
172 L/min
53 L/min
41 L/min
WTP
(d)
Caliper log (mm)
6.3m
To max GWL
120 140 160
min GWL
Depth (m bgl)
(e)
Upward velocity(m/min)
0.0 0.5 1.0
Pt. injection @ 33.5 mbgl
Pt. injection @ 39.5 mbgl
Velocity
mass remaining
0 50 100
% of NaCl remaining
(f)
GWL @ time of test
Main zone of diffuse outflow
Upward flow with minor diffuse outflow
Crossflow, but adding flows to upward
from below depth interval
Upward flow zone
Major inflowing feature with
outflow and upflow component
Weak diffuse crossflow features
Stagnant well bottom marked
by iron staining
6 L/min
8 L/min
11 L/min
4 L/min

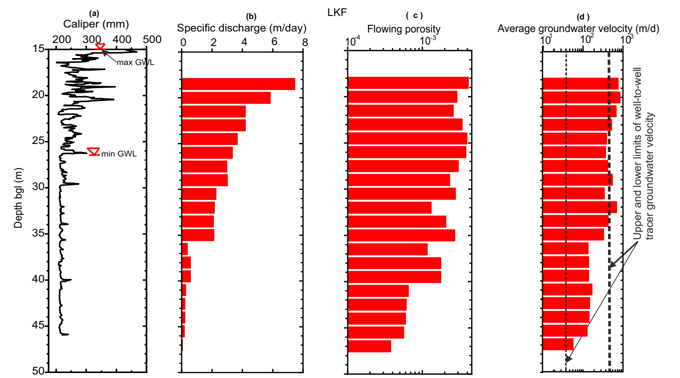
LKF
(a)
Caliper (mm)
max GWL
min GWL
Depth bgl (m)
(b)
Specific discharge (m/day)
(c)
Flowing porosity
(d)
Average groundwater velocity (m/d)
Upper and lower limits of well-to-well tracer groundwater velocity